AVE Trends in Intelligent Energy Letters

AVE TRENDS PUBLICATIONS

A Non-Isolated High-Gain DC-DC Converter with Z-Quasi Resonant Network for Electric Vehicle Battery Charging Applications

P. Srinivasan[1,*], K. Arulvendhan[2], Amal Babu[3], S. Silvia Priscila[4], Dilli Kasi Rao Kotha[5]

[1]Department of Electrical and Electronics Engineering, Saveetha Engineering College, Chennai, Tamil Nadu, India.
[2,3]Department of Electrical and Electronics Engineering, SRM Institute of Science and Technology, Ramapuram, Chennai, Tamil Nadu, India.
[4]Department of Computer Science, Bharath Institute of Higher Education and Research, Chennai, Tamil Nadu, India.
[5]Faculty of Engineering, Environment and Computing, Coventry University, Coventry, England, United Kingdom.
srinivasp808@gmail.com[1], arulvenk@srmist.edu.in[2], amal.babu35@gmail.com[3], silviaprisila.cbcs.cs@bharathuniv.ac.in[4], kothad@coventry.ac.uk[5]

*Corresponding author

Abstract: A non-isolated high-step-up DC-DC converter using the classic boost architecture is proposed in this study, functioning continuously in input-current mode. Low efficiency, complex control, and discontinuous current plague conventional voltage multiplier converters (VMCs). An interactive ZQR (Z-Quasi Resonant) network boosts voltage gain to improve stability. The high-side switch circuit design uses a single high-side switch to simplify driving circuitry and produce high gain using a single MOSFET and five diodes, reducing component count and system cost. A complete theoretical examination of ideal and non-ideal CCM operation was done. CCM operating conditions, voltage gain, and efficiency sensitivities are defined in the study, along with comparative charts showing performance across different parameters. In addition to the non-isolated design, this section covers an isolated bipolar DC-DC converter for energy storage integration in EV charging systems. This structure provides decoupled bipolar outputs for balanced, efficient, and stable EV battery charging, prolonging battery life and enhancing charging dependability. A PIC16F84A microcontroller-based hardware implementation with accurate switching pulses is described for power conversion and maximum performance. The recommended converters for next-generation EV charging technologies have high gain, ease of construction, and stable isolated operation, demonstrating their viability.

Keywords: EV Charging Systems; Component Count; Voltage Multiplier Converter (VMC); Bipolar Isolated Converter; Electric Vehicles; Hardware Implementation; Power Conversion.

Cite as: P. Srinivasan, K. Arulvendhan, A. Babu, S. S. Priscila, and D. K. R. Kotha, “A Non-Isolated High-Gain DC-DC Converter with Z-Quasi Resonant Network for Electric Vehicle Battery Charging Applications,” *AVE Trends in Intelligent Energy Letters*, vol. 1, no. 2, pp. 71–86, 2025.

Journal Homepage: https://www.avepubs.com/user/journals/details/ATIEL

Received on: 04/11/2024, **Revised on:** 23/12/2024, **Accepted on:** 29/01/2025, **Published on:** 09/12/2025

DOI: https://doi.org/10.64091/ATIEL.2025.000187

1. Introduction

With the rapid advancement of power electronics, the need for efficient, small, and dependable DC-DC converters in renewable energy systems, electric vehicles (EVs), and microgrid applications has increased significantly. In this scenario, high-gain DC-

DC converters are required to convert a small amount of energy at one input voltage level to the higher voltage required by loads or storage devices in the sectors. Take EV battery charging or energy storage integration, for instance: it is not only required that the converters have a high voltage gain, but that they also meet requirements for reliability, compactness, and efficiency. Meeting these requirements, however, has proven difficult, as it also requires trade-offs among voltage gain, device stress, the number of components used, and system performance. There are two main classes of DC-DC converters: isolated and non-isolated. There are also non-isolated converters that use a high-frequency transformer to control the voltage gain via the transformer's turn ratio. This property makes them very attractive to applications that require galvanic isolation, such as microgrids and EV systems. The transformer also shields loads from input-source faults, enhancing safety and efficiency in step-up applications. However, transformers introduce serious drawbacks, and the logic circuits are large, power-dense, and expensive. Moreover, suppressing loads such as leakage inductance and parasitic effects increases circuit complexity and raises reliability concerns.

Therefore, although isolation converters are essential for some applications, due to their limitations, non-isolation converters are of interest, particularly when power density and small size are required [1]. Among these non-isolated topologies, the boost converter is the simplest and most common. This maintains a constant current into the input, reducing current stress on the input filter capacitor and improving reliability. Conventionally, a low-side MOSFET is used in the boost converter to simplify the driving circuit. However, these benefits come at the cost of a voltage gain that heavily relies on the duty cycle in a standard boost converter. Though it generates a high output voltage at low duty cycles, the maximum voltage gain is limited. So, it is not suitable for a high step-up application. To overcome this limitation, many modifications and new topologies were proposed. A specific class of topologies is the so-called quadratic boost converter, which, in theory, offers a squared voltage gain compared to the classical boost design. Although the quadratic converters may double the input voltage at the output, they are not free of disadvantages. Some of these include a lack of a common input-output ground, increased input current ripple, and heavy voltage stress in some semiconductor devices. For example, in most quadratic topologies, the second diode experiences greater output-voltage stress, requiring high-voltage-rated components. In addition, quadratic topologies will likely require two switches, thereby complicating the scheme and reducing overall reliability [2].

Others use three inductors, which increases bulk and expense but does not yet achieve the needed voltage gain at appropriate duty cycles. To address these challenges, researchers developed complex one-switch topologies that achieved double the voltage gain of quadratic converters. For instance, some designs have achieved an 8-fold gain at 50% duty cycle, exceeding those of conventional quadratic solutions. Such topologies, however, are typically characterised by high input current ripple, leading to low efficiency and increased input capacitor stress. Other approaches, including the use of boost converters with super-lift Luo or the buck-boost topologies combined, have also been investigated. The hybrid circuits use voltage-lift principles to achieve gain extension but are typically two-switch-based, which again leads to reliability issues and increased control complexity.

Semiconductors are often also subjected to voltages exceeding the output voltage, requiring more resilient devices that raise costs and limit practical use. The second promising area is the hybridisation of the boost and SEPIC topologies, which can achieve high gains while maintaining continuous input current. Yet, such methods typically use three inductors and a combination of passive components, leading to higher bulk and lower power density [3]. Further, their performance at moderate duty cycles continues to lag behind next-generation requirements for high-gain applications, especially in EV systems where compactness and reliability matter. Given these limits, the current study proposes a novel non-isolated high-gain converter that addresses the shortcomings of previous topologies.

The new architecture has one switch, three inductors, five diodes, and three capacitors. Establishing a common ground point between the source and load allows a continuous input current waveform, reducing ripple current and input filter capacitor stress. Unlike traditional low-side-switched boost converters, this configuration employs a high-side switch but with a relatively straightforward driver circuit. The method achieves 8× voltage gain at 50% duty cycle, approximately doubling the gain of traditional quadratic boost converters without requiring multi-switched or transformer-based circuits. The most vital aspect of the given topology is the use of a Z-Quasi Resonant (ZQR) network, seamlessly integrated into the design. The incorporation of the ZQR network reduces device voltage stress, eliminates unwanted transients, and improves converter reliability.

The inclusion helps smooth operation in continuous conduction mode (CCM), which is required to achieve high efficiency and minimise component stress [4]. In addition, the ZQR network reduces the negative impact of high input current ripple, making the converter optimal for sensitive applications such as EV battery charging and renewable energy systems. The innovation in this research is not only the compact one-switch configuration and enhanced voltage gain, but also the balanced trade-offs among efficiency, reliability, and power density. The suggested converter breaks the limits of quadratic and hybrid topologies by achieving high gain at moderate duty cycles without a large structure. It thus constitutes an appealing solution for efficient, lightweight, and robust high-gain conversion applications.

2. Literature Review

This study focuses on the Z-Quasi Resonant (ZQR) network, a multi-port, non-isolated (dual-input, single-output) DC/DC power electronic interface. The converter handles both grid and PV input sources [5]. The ZQR network employing the proposed DC/DC converter has zero-current turn-on, high voltage gain, and low voltage stress on converter switches at up to 40% duty ratio, with fewer switches than standard DC/DC converters. The converter has the above-mentioned capability, allowing it to be used in situations where a high voltage gain is required for off-board charging of an EV (electric vehicle). More input and output ports might be added to the suggested multi-port ZQR converter without reducing its efficiency or gain. Even if one of the charging sources fails, the intended converter will continue to operate. Using the basic laws governing converter performance, the proposed converter is mathematically modelled and tested in MATLAB/Simulink under a range of operating conditions. This paper also includes a comparison of the constructed multiport ZQR DC/DC converter with topologies reported in the literature, as well as a thorough study of both steady-state and dynamic performance. A 300 W prototype unit with a switching frequency of 20 kHz was built to test the proposed converter's efficacy. The experimental findings validate the theoretical study's efficacy, the previously mentioned benefits, and the features of the proposed multiport ZQR DC/DC converter. In Choudhary and Elangovan [6] and Khan and Thakre [7], high-step-up dc-dc converters are needed to control power flow in photovoltaic (PV) systems.

In transformer-less topologies, dc-dc converters with high voltage gain are the answer, since the output voltage of solar sources is lower than the grid voltage. The topology being discussed is intended for use in unfolding inverters and current-source inverters (CSI). Furthermore, theoretical analysis is verified using a 200W prototype. Finally, to confirm its use in unfolding inverters, a dc rectified sinusoidal output current modulation is carried out. In [8], Anto and Sunny proposed a current-fed resonant inverter. The high-voltage transformer's step-up ratio is kept very low to reduce the effects of its leakage inductance and other nonidealities. Additionally, to achieve a soft-switched conversion, the parasitic capacitance of the HV transformer and switches, as well as the leakage inductance, are employed as resonant components. ZCS, which operates over a broad load range, is used to gently switch the switches. The transformer's secondary side uses a collection of Cockroft-Walton multipliers to achieve the desired result. The X-ray machine requires 100kV and 2.5 mA, which the converter achieves by operating at 100 kHz with overlap-time switching. This paper presents a methodically detailed analysis of selecting each discrete component in this architecture [9]. In Kjaer et al. [10], a high-voltage-gain method using dc-dc power converters is proposed. The proposed topologies can draw continuous current from two input sources and function as multiport converters. Additionally, they can interleave a continuous current from a single source. The suggested converter can easily achieve a constant input current and a gain of 12. An individual PV panel can be connected to a 100 V_{DC} bus using such a converter.

To validate the analytical results, a prototype has been created, and the design and component selection processes have been detailed. In Ahmadi et al. [11], non-isolated boost interleaved converters operate in parallel to achieve a high step-up gain without requiring high-duty-ratio operation. From the specified input sources, a continuous current can be extracted in an interleaved fashion. This converter can reduce current stress and input current ripple, extending the lifespan of the input source and lowering conduction losses. Because of these benefits, it is attractive for sustainable applications such as microgrids and solar systems. In a microgrid system, they can also be used to interface the 400 V_{DC} bus with low-voltage sources such as photovoltaic (PV) panels, batteries, and fuel cells. In Ahmadi et al. [12], by combining active clamping and quasi-resonant approaches, the suggested converter can achieve ZVS operation for each switch. Compared to its competitors, the suggested converter has fewer switches because it does not need a transformer to achieve high gain. As a result, it is more cost-effective and more reliable. Additionally, conduction loss is significantly reduced because the proposed converter uses only four switches per mode. It also offers superior voltage matching, unlike its isolated equivalents, which employ the phase-shift technique. As a result, isolated converters inherently lack the circulating current, leading to current stress and loss [13]. To illustrate the converter's performance across various modes, simulations for each mode are conducted, and the switching strategy is provided. The impacts of the suggested converter are demonstrated by the efficiency calculations and simulation results [14].

3. Methodology

A High-Gain Dual Z-Quasi Resonant (ZQR) DC-DC Converter for Off-Board EV Charging is presented in this study. The block diagram in Figure 1 presents a smart DC-DC battery charging system comprising a DC supply, a DC-DC converter (ZQR), a driver circuit (IR2110), and a PIC16F84A microcontroller, interfaced with a battery as the final output. The DC supply delivers the essential input voltage, which is structured by the DC-DC converter; this converter performs essential voltage conversion and current management, ensuring safe and efficient battery charging while protecting against damage from variable input conditions. Critical to the converter’s operation is the IR2110 driver circuit, which delivers precise gate-control signals to the power switches via pulse-width modulation (PWM), enabling high-speed switching and improved system efficiency. The driver receives control commands from a PIC16F84A microcontroller, which acts as the system’s intelligence hub. The microcontroller is programmed to monitor charging constraints, including input and output voltages and currents, and the battery state; it makes real-time decisions to adjust the PWM signals, dynamically optimising the charging process, prolonging battery life, and protecting against overcharging. The circuit shown in Figure 2 represents the proposed non-isolated high-gain DC–DC converter incorporating a single switch, three capacitors, three diodes, and an inductor.

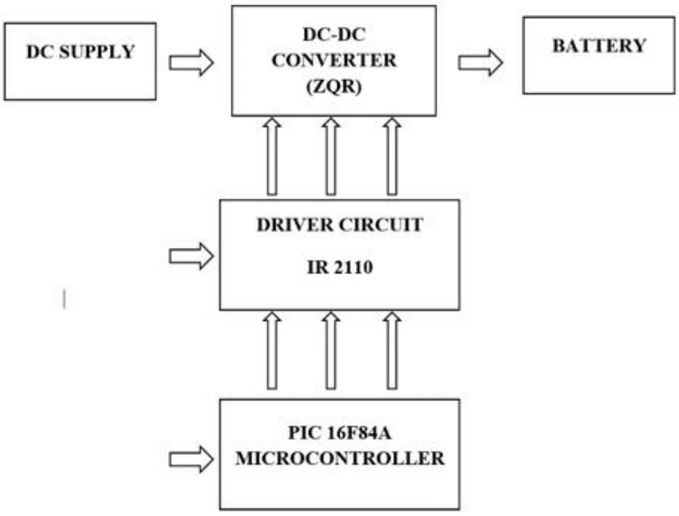

Figure 1: Block diagram of the proposed system

The design is derived from a boost topology, enhanced with a voltage-lift technique and a diode–capacitor network to achieve higher voltage gain.

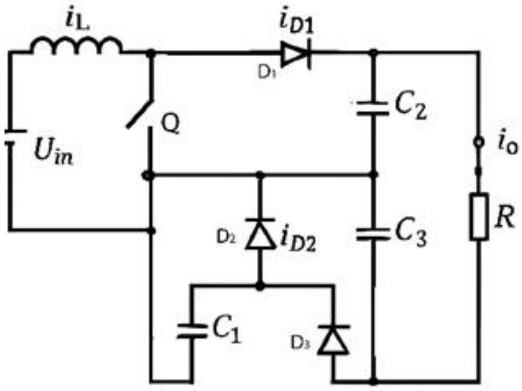

Figure 2: Circuit diagram for dual Z-quasi resonant converter (ZQR)

The operation can be divided into two modes:

- **Switch ON Mode (Q conducting):** When the MOSFET switch Q is turned on, the input inductor L stores energy from the source Uin. During this period, diodes D1, D2, and D3 become forward-biased, allowing capacitors C1, C2, and C3 to charge. The input current is continuous, reducing stress on the input capacitor and improving stability.
- **Switch OFF Mode (Q off):** When the switch Q is turned off, the stored energy in the inductor is released through the diode–capacitor network. The charged capacitors are stacked in series, transferring their stored energy to the load R. This series charging–discharging action produces a boosted output voltage Uo, which is significantly higher than the input voltage Uin.

The integration of multiple capacitors and diodes ensures ripple reduction, higher gain, and continuous input current. At 50% duty cycle, the converter achieves nearly twice the gain of conventional quadratic boost converters while maintaining a single active switch, thereby improving efficiency and reliability.

4. Simulation Results and Discussion

The circuit diagram for a conventional new high-gain single ZQR DC-DC converter system is displayed in Figure 3.

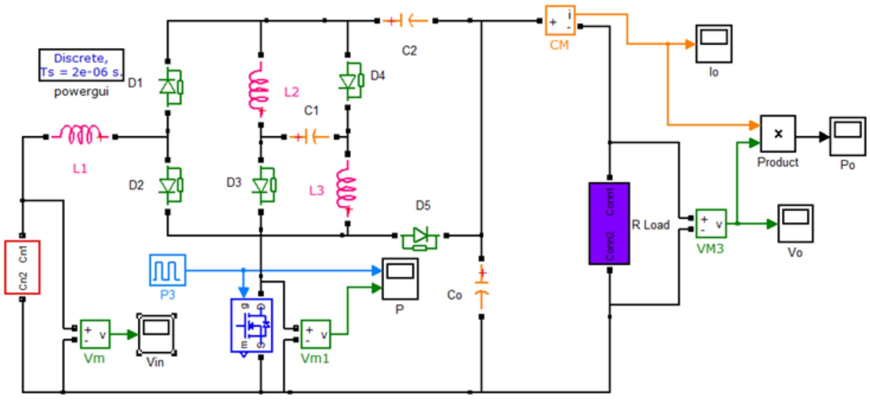

Figure 3: Simulation of open-loop high-gain single ZQR DC-DC converter system

The applied required voltage of 15V is displayed in Figure 4.

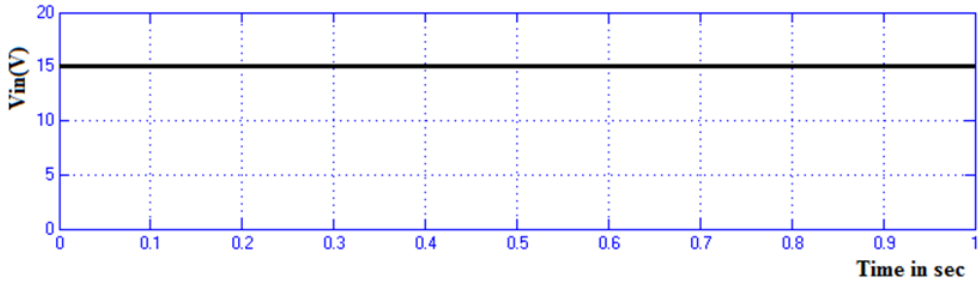

Figure 4: Input supply voltage

The switching pulse for the new high-gain single ZQR DC-DC converter and the Vds waveform, with values of 1V and 100V, respectively, are illustrated in Figure 5.

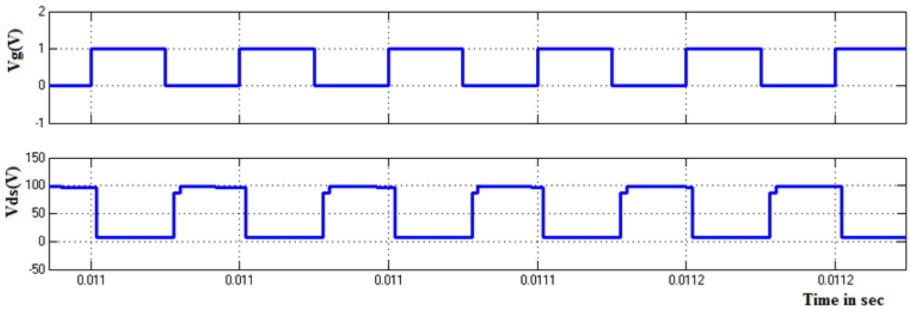

Figure 5: High-gain single ZQR DC-DC converter and V_g and V_{DS}

The output voltage across the load, 86V, is displayed in Figure 6.

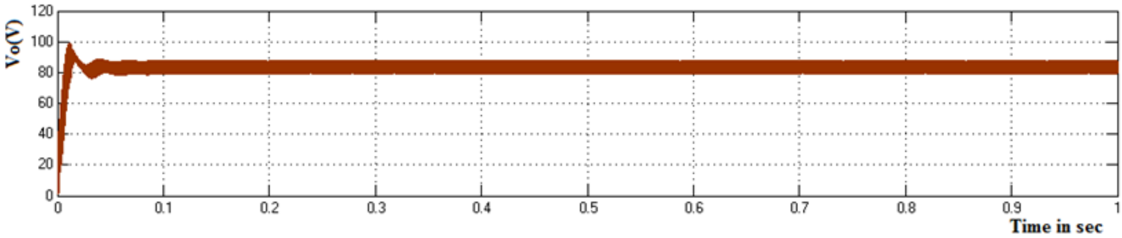

Figure 6: Output voltage of the load

The output ripple voltage across the R-load is 6 V, as seen in Figure 7.

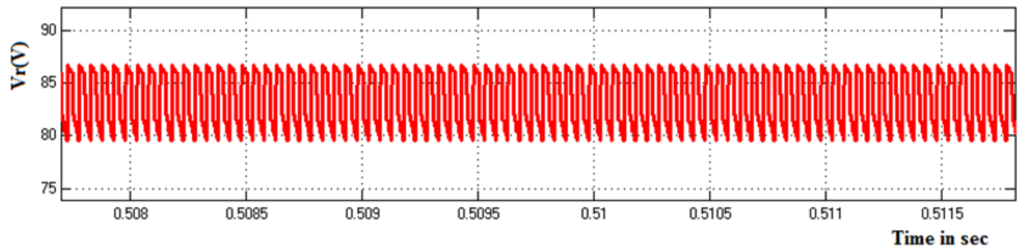

Figure 7: Output ripple voltage of the load

Figure 8 shows the load current at 1.7A.

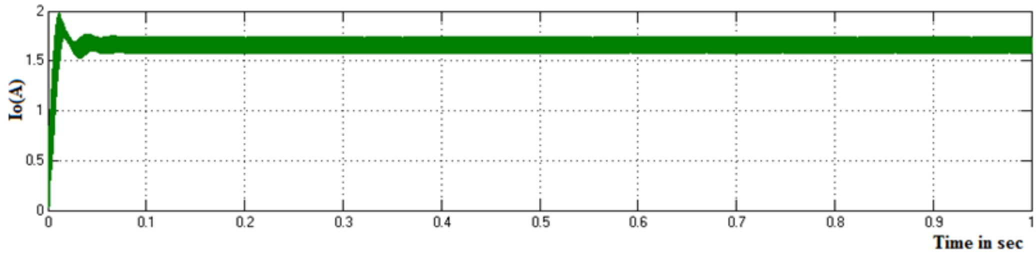

Figure 8: Output current of the load

Figure 9 shows the output ripple current through the load, which is 0.16A.

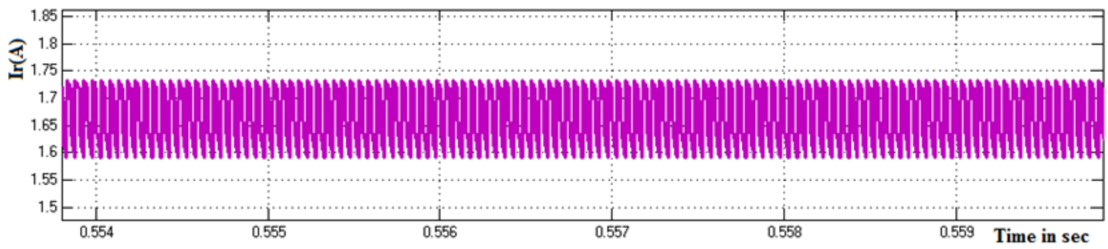

Figure 9: Output ripple current through the load

Figure 10 shows the 150W output power.

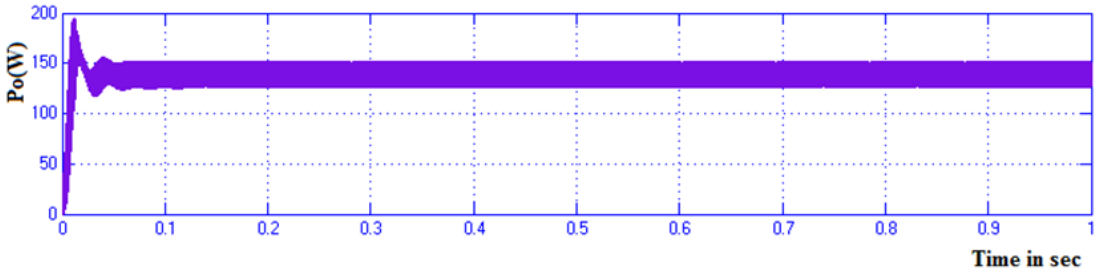

Figure 10: Output power

Figure 11 shows the output ripple power, which is 25W.

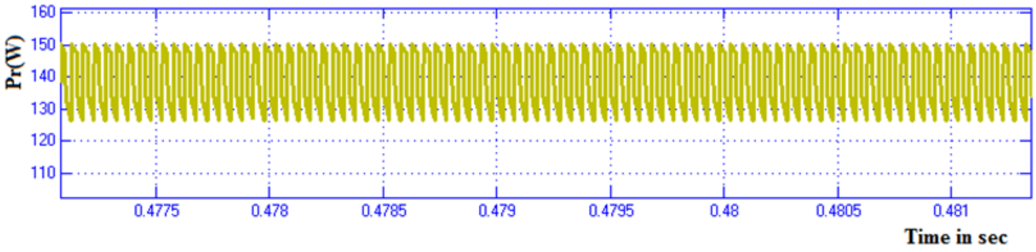

Figure 11: Output ripple power

The projected innovative high-gain single DC-DC converter ZQR system's circuit diagram is displayed in Figure 12.

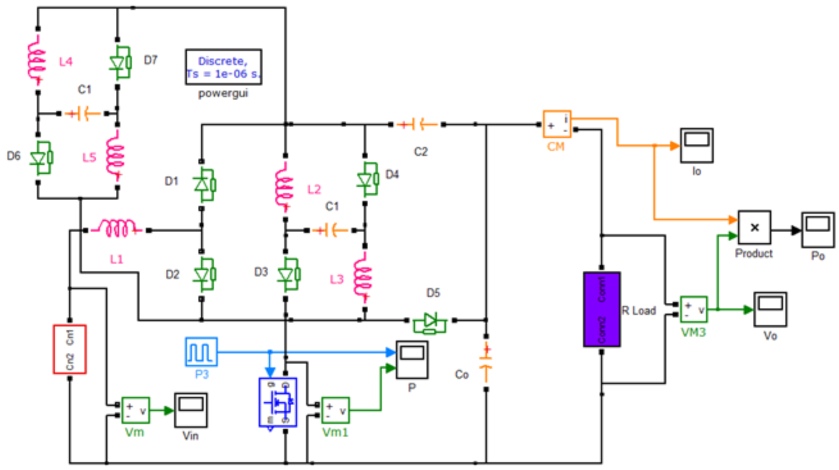

Figure 12: Proposed ZQR DC-DC converter high-gain dual system

Figure 13 displays the input voltage, which is 15V.

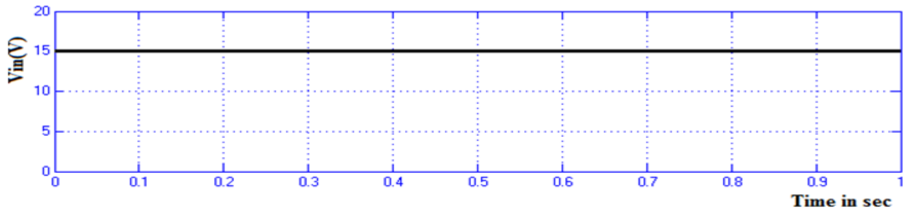

Figure 13: Input voltage

For the revolutionary high-gain single ZQR DC-DC converter, switching pulses of 1V and 125V are displayed in Figure 14.

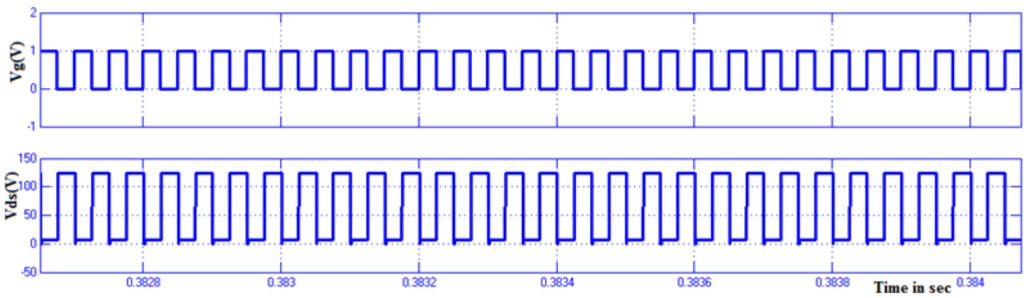

Figure 14: Switching pulse for M1 and V_{DS}

Figure 15 displays the output voltage across the load, which is 123V.

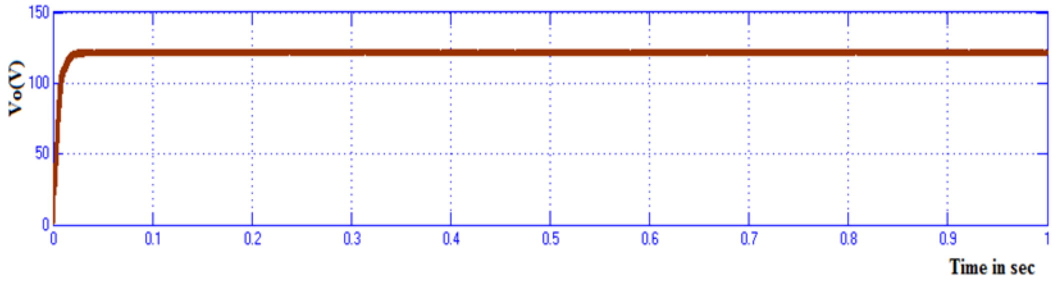

Figure 15: Output voltage across the load

As illustrated in Figure 16, the output ripple voltage over R-load is 2.5 V.

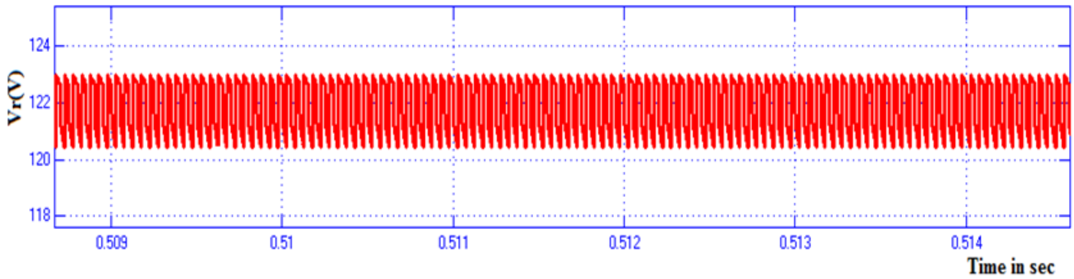

Figure 16: Output ripple voltage across the load

In Figure 17, the output current through the load is shown as 2.5A.

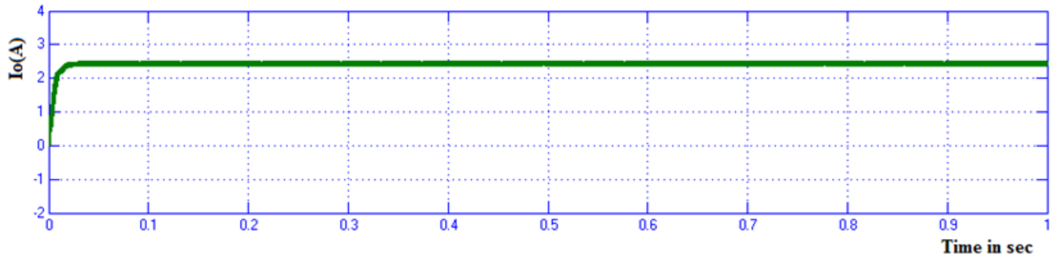

Figure 17: Output current through the load

Figure 18 shows that the output ripple current through the load is 0.05A.

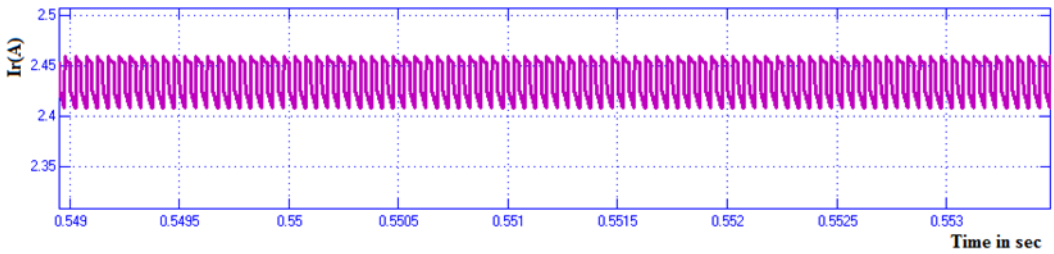

Figure 18: Output ripple current through the load

In Figure 19, the output power is 300W.

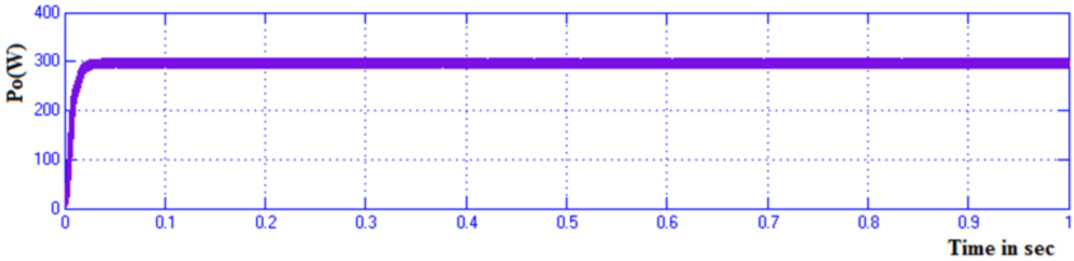

Figure 19: Output power

15W is the output ripple power, which is illustrated in Figure 20.

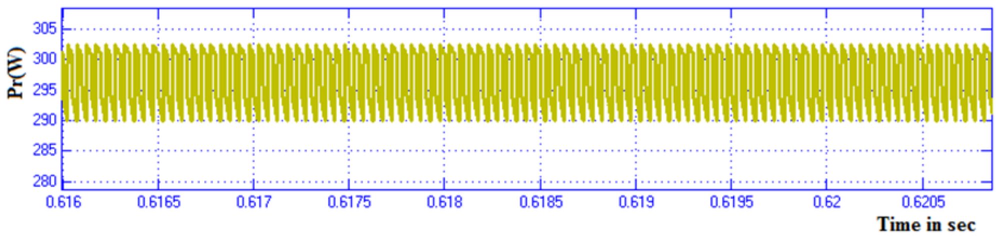

Figure 20: Output ripple power

Table 1 shows the Comparison of output current, output power, and output voltage for the conventional and proposed Novel high-gain ZQR system.

Table 1: Comparison of output voltage, current, and power

DC-DC Converter	Vo(V)	Io(A)	Po(W)
Novel high-gain single ZQR	86	1.7	150
Novel high-gain dual ZQR	123	2.5	300

Figure 21 shows the bar chart comparing the output current, output power, and output voltage for the conventional and proposed novel high-gain ZQR system.

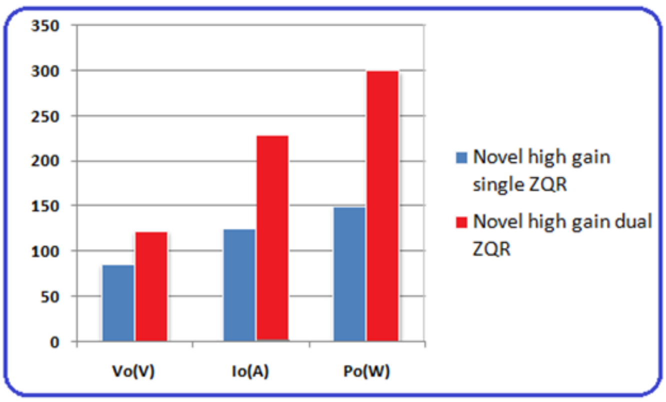

Figure 21: Comparison of output voltage, current, and power

From the above Table results, it is clear that the output voltage is improved from 86 V to 123 V; the output current is improved from 1.7 A to 2.5 A; the output power is improved from 150 W to 300 W. Hence, the proposed novel high-gain dual ZQR system has better performance than the conventional high-gain single ZQR system. Table 2 compares the output ripple voltage, output ripple current, and output ripple power of the proposed novel high-gain ZQR system with those of the conventional system.

Table 2: Comparison of output ripple voltage, output ripple current, and output ripple power

DC-DC Converter	Vr(V)	Ir(A)	Pr(W)
Novel high-gain single ZQR	6	0.16	25
Novel high-gain dual ZQR	2.5	0.05	15

Figure 22 displays a bar chart comparing the output ripple voltage, output ripple current, and output ripple power of the proposed novel high-gain ZQR system with those of the conventional system.

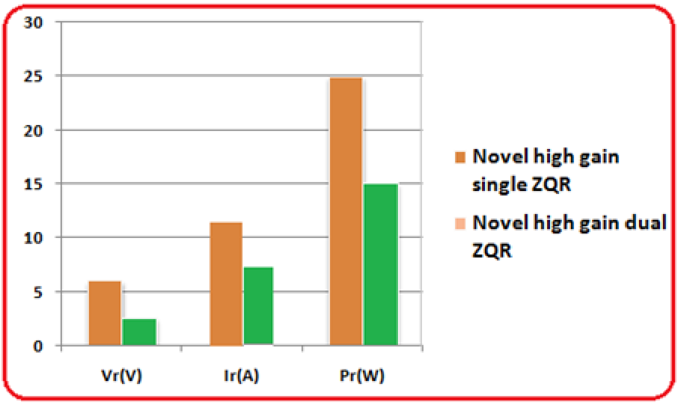

Figure 22: Output comparison of ripple voltage, output ripple current, and ripple power output

The output ripple power is reduced from 25 W to 15 W, the output ripple voltage is reduced from 6 V to 2.5 V, and the current is reduced from 0.16 A to 0.05 A. Therefore, compared to the traditional high-gain single ZQR system, the proposed high-gain dual ZQR system performs better.

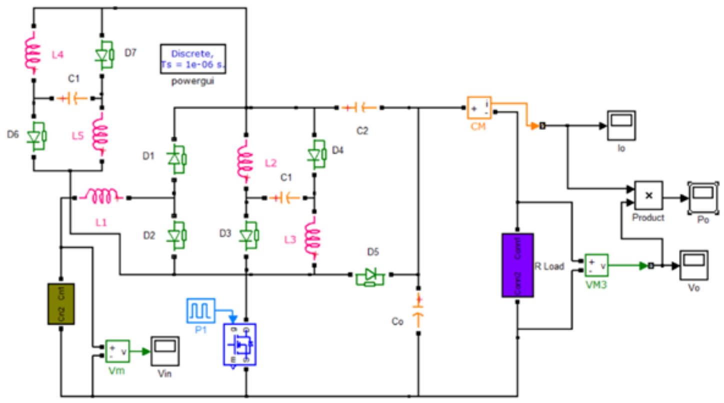

Figure 23: Simulation of closed-loop ZQR DC-DC converter high-gain dual with source disturbance

The circuit diagram of the novel high-gain dual ZQR DC-DC converter with source disturbance is shown in Figure 23. The voltage input is shown in Figure 24 at 15V.

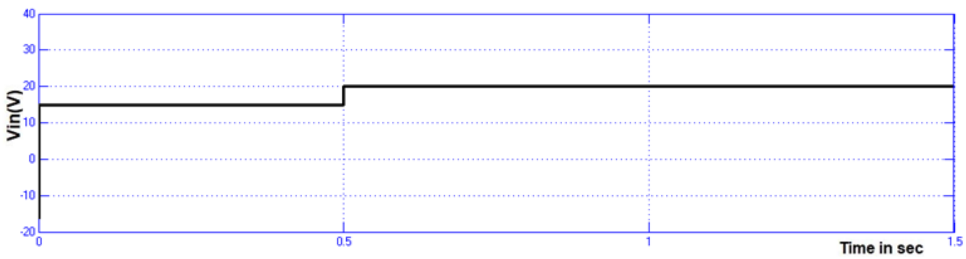

Figure 24: Input voltage

The output R-Load voltage across is given in Figure 25, and the rate is 162V.

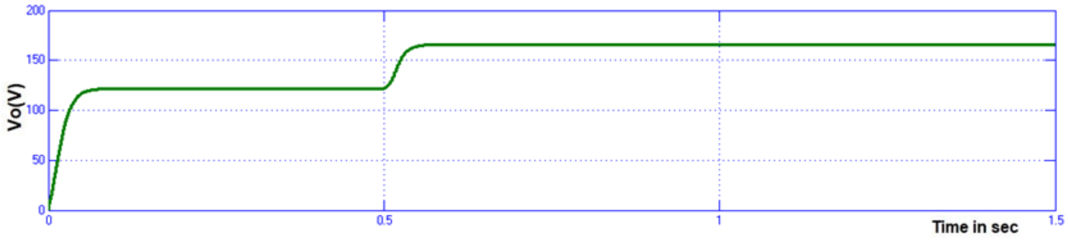

Figure 25: Voltage across R- load

The current through R-Load is shown in Figure 26 and is 3.2A.

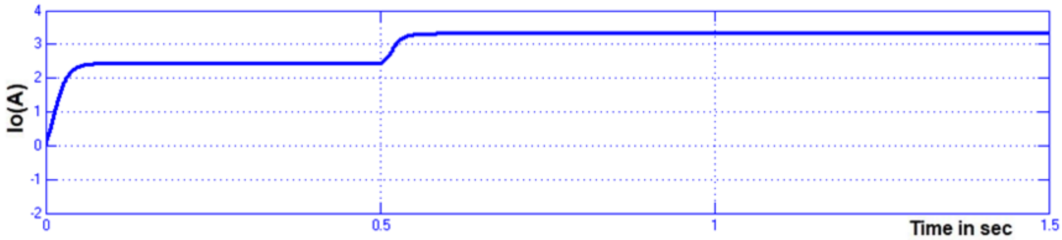

Figure 26: Current through R- load

The output power is shown in Figure 27 and is 580W.

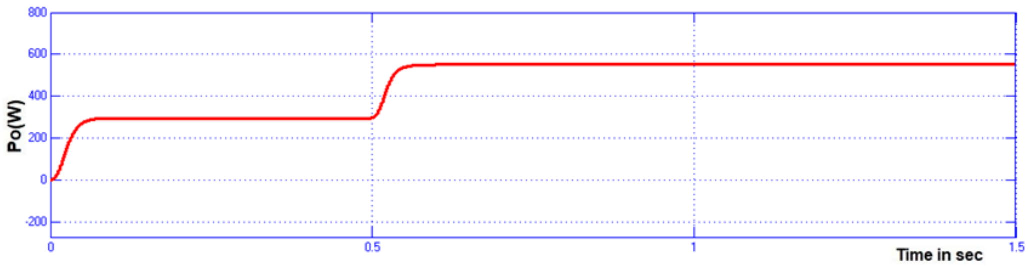

Figure 27: Output power

The circuit diagram of the novel ZQR DC-DC converter, a high-gain dual with a closed-loop PI controller, is shown in Figure 28.

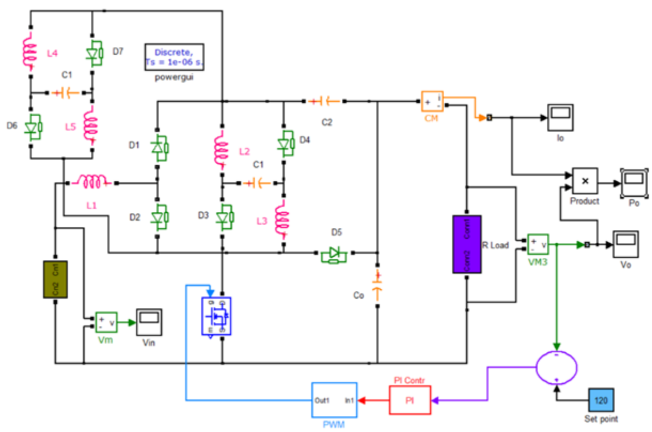

Figure 28: Circuit diagram of ZQR DC-DC converter, novel high-gain dual with closed-loop PI controller

The input voltage is shown in Figure 29 and is 15V.

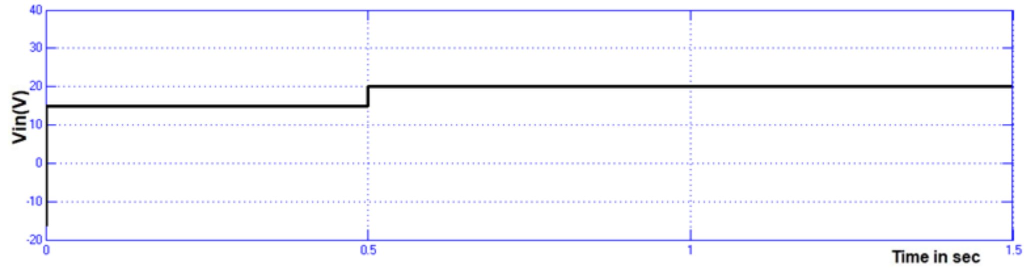

Figure 29: Input voltage

The R-Load output voltage across is shown in Figure 30, and the rate is 123V.

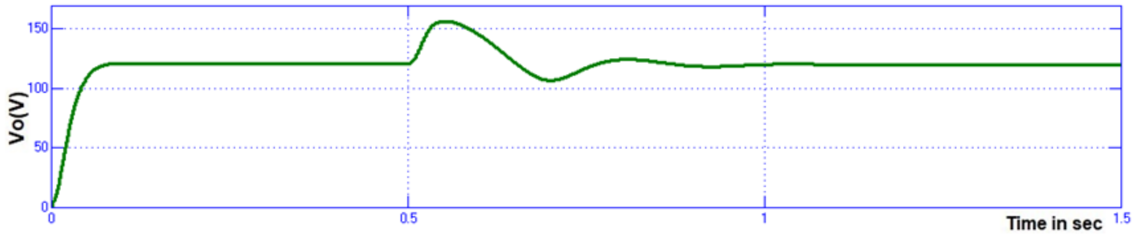

Figure 30: Voltage across R load

The output current through R-Load is shown in Figure 31 and is 2.5A.

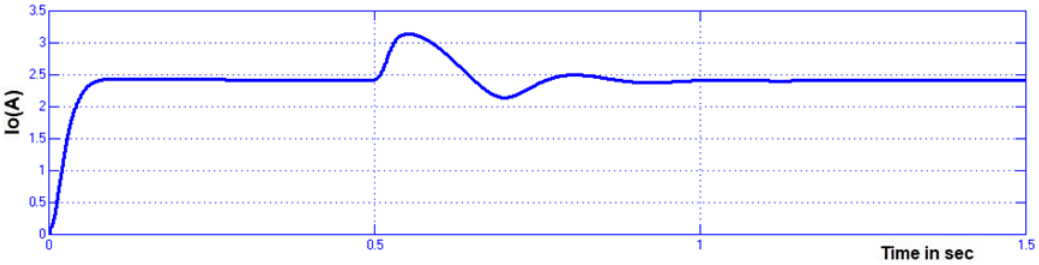

Figure 31: Current through R- load

The output power is exposed in Figure 32, and the value is 300W.

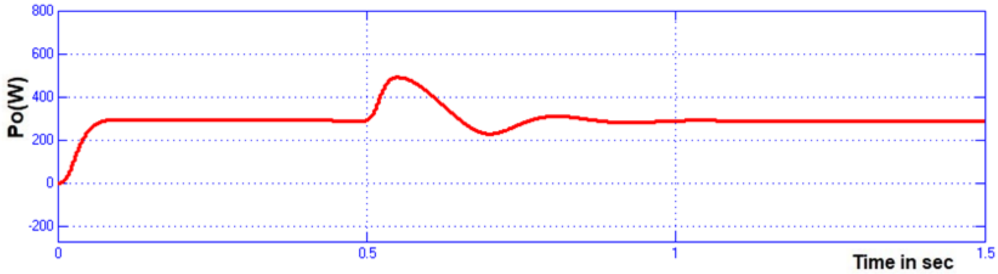

Figure 32: Output power

The circuit diagram of the novel ZQR DC-DC converter, featuring a high-gain dual with a closed-loop FOPID controller, is shown in Figure 33.

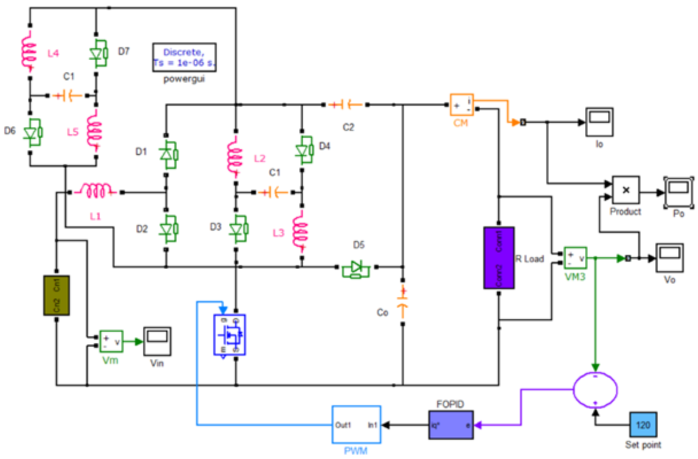

Figure 33: Simulation diagram of ZQR DC-DC Converter high gain dual with closed loop FOPID controller

The input voltage is shown in Figure 34 and is 15V.

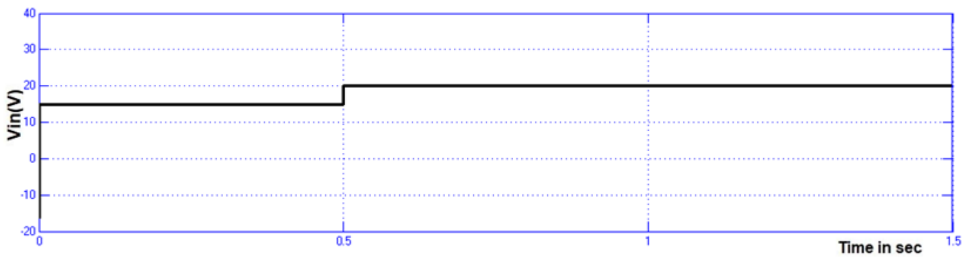

Figure 34: Input voltage

The output R-Load voltage across is shown in Figure 35, and the rate is 123V.

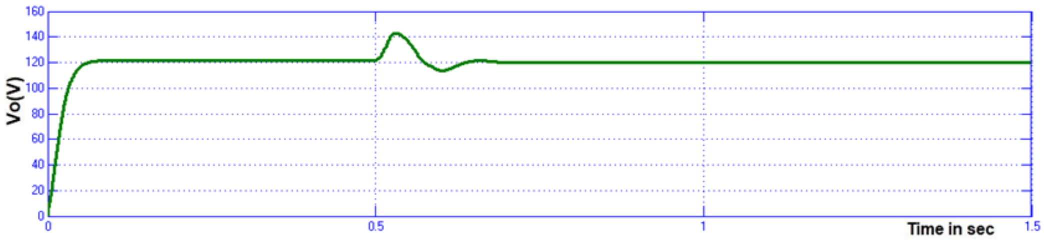

Figure 35: Voltage across R- load

The output current through R-Load is shown in Figure 36, and it is 2.5A.

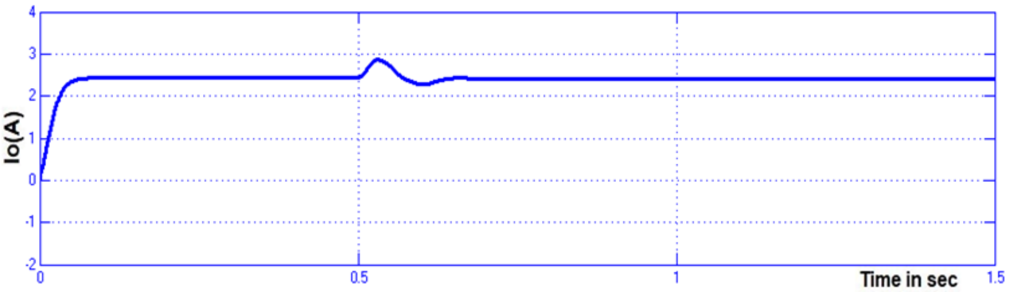

Figure 36: Current through R- load

The output power is exposed in Figure 37, and the value is 300W.

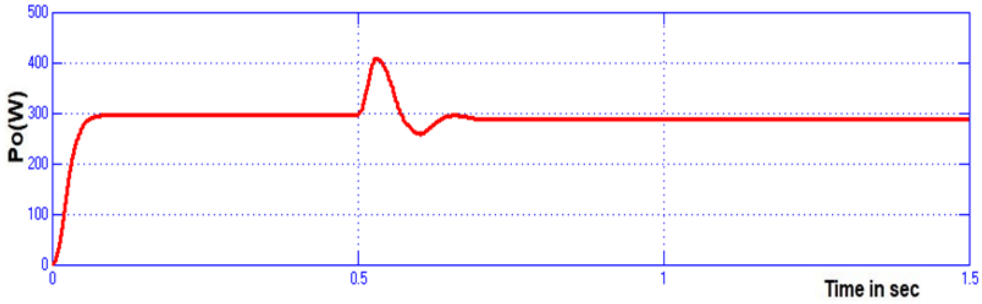

Figure 37: Output power

Table 3 compares the time-domain characteristics of a unique high-gain dual ZQR DC-DC converter with closed-loop FOPID and PI controllers.

Table 3: Comparison of time domain parameters

Types of controllers	Tr	Tp	Ts	Ess
PI	0.54	0.56	1	2.23
FOPID	0.52	0.54	0.72	1.56

The bar chart comparing the closed-loop performance of the novel high-gain dual ZQR DC-DC converter with PI and FOPID controllers is shown in Figure 38.

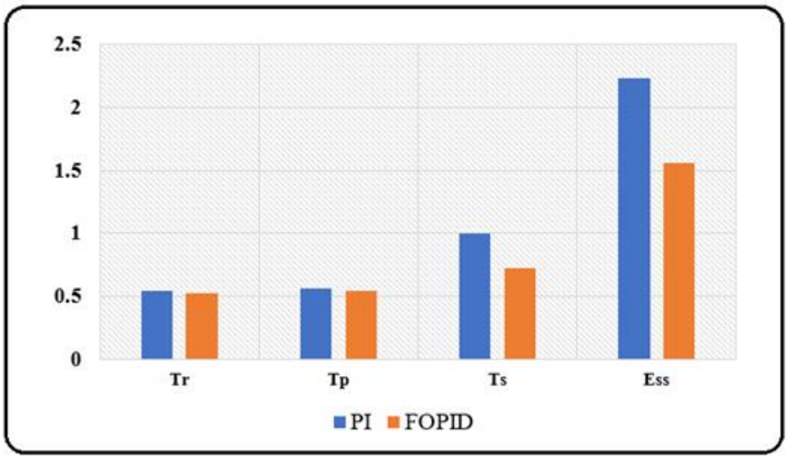

Figure 38: Comparison of time domain parameters

From Table 3, it is evident that time domain parameters of rise time, peek time, settling time and steady state error voltage with respect to output voltage is reduced by FOPID, hence FOPID has better performance than PI controller of ZQR DC-DC converter novel high gain dual system.

5. Hardware Implementation and Discussion

The proposed dual ZQR high-gain DC-DC converter system was developed and tested using a hardware prototype, as shown in Figure 39. The setup consists of the following functional blocks: AC–DC rectifier, regulator circuit, PI controller, driver circuit, dual ZQR networks, DC–DC converter stage, and R-load. Each module is interconnected to ensure smooth power flow, closed-loop regulation, and high-gain voltage conversion. System operation begins with the AC–DC rectifier, which converts the 230 V AC supply to a regulated DC input. The rectified voltage is then processed by the regulator circuit, which stabilises the DC supply for the control and driver circuits. The PI controller generates appropriate control signals to regulate output voltage, while the driver circuit amplifies and conditions these signals for the MOSFET switch in the converter stage. The core power conversion occurs in the dual Z-Quasi Resonant (ZQR) networks, which are cascaded with the main DC–DC converter.

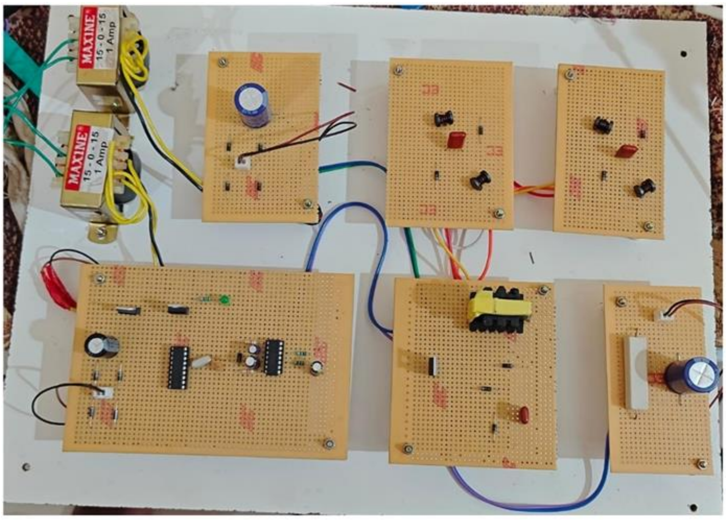

Figure 39: Proposed hardware model

These networks play a crucial role in achieving higher voltage gain, reducing switching stress, and ensuring continuous input current. The integration of dual ZQR circuits effectively doubles the gain achieved in conventional single ZQR configurations while also minimising ripple components. The R-load, which is the load from which experimental measurements are extracted, is fed by the DC–DC converter output. Hardware results confirm that the proposed dual ZQR system outperforms the single ZQR system. In particular, the prototype demonstrated an output voltage of 123 V, an output current of 2.5 A, and an output power of 300 W, with very low output voltage ripple (2.5 V), output current ripple (0.05 A), and output power ripple (15 W). The hardware implementation was used to validate the effectiveness of the proposed topology, and it was found that the dual ZQR DC-DC converter exhibits high voltage gain, improves conversion efficiency, and operates the second-stage rectifier with low ripple, making it a viable candidate for renewable energy conversion systems and EV charging applications.

6. Conclusion

In this work, a new high-step-up-gain dual ZQR DC-DC converter model is simulated and analysed to evaluate its performance. Comparison with a basic single-ZQR structure also revealed that the output voltage, current, and power were enhanced. The output voltage magnification of the proposed dual ZQR system was improved from 86 V to 123 V. Output current was enhanced from 1.7 A to 2.5 A and the output power was raised from 150 W to 300 W, Secondly, it could be testified that the output ripple voltage was effectively observed from 6 V to 2.5 V, the ripple current was reduced from 0.16 A to 0.05 A and the ripple power was improved from 25 W to 15 W, which proved the better efficiency and stability. To improve performance, closed-loop control techniques were also applied to the dual-ZQR converter. In a comparison study of FOPID control versus PI controllers, FOPID was reported to provide improved dynamic response. The FOPID controller, in particular, decreased the rise time (0.54 s to 0.52 s), peak time (0.56 s to 0.54 s), settling time (1.0 s to 0.72 s), and steady-state error (2.23 V to 1.56 V). The proposed dual ZQR DC-DC converter with FOPID control provides better gain, ripple factor, and transient response, making it a suitable candidate for renewable energy systems and EV charging applications.

Acknowledgement: The authors sincerely acknowledge Saveetha Engineering College and SRM Institute of Science and Technology for providing an encouraging academic environment and essential resources. Their continuous support and guidance played a vital role in the successful completion of this work.

Data Availability Statement: The data used in this study are derived from the study of a non-isolated high-gain DC–DC converter incorporating a Z-quasi-resonant network for electric vehicle battery charging applications. The dataset supporting the findings of this study is available from the corresponding authors upon reasonable request.

Funding Statement: This research was conducted without any external financial support from public, commercial, or non-profit funding agencies.

Conflicts of Interest Statement: The authors declare that there are no conflicts of interest associated with this work. All sources of information have been appropriately acknowledged and cited.

Ethics and Consent Statement: The study adhered to ethical standards, with required approvals obtained and informed consent secured from all participants.

References

1. Y. Zhang, Y. Mou, and Y. Yang, "An energy management study on hybrid power of electric vehicle based on aluminium air fuel cell," *IEEE Transactions on Applied Superconductivity*, vol. 26, no. 7, pp. 1-6, 2016.
2. T. Yuvaraj, K. R. Devabalaji, J. A. Kumar, S. B. Thanikanti, and N. I. Nwulu, "A comprehensive review and analysis of the allocation of electric vehicle charging stations in distribution networks," *IEEE Access*, vol. 12, no. 1, pp. 5404–5461, 2024.
3. M. P. Suresh, S. J. Isac, M. Joly, and J. A. Kumar, "Automatic fault detection and stability management using intelligent hybrid controller," *Electric Power Systems Research*, vol. 238, no. 1, p. 111075, 2025.
4. S. Harini, N. Chellammal, B. Chokkalingam, and L. Mihet-Popa, "A novel high gain dual input single output Z-quasi resonant (ZQR) DC/DC converter for off-board EV charging," *IEEE Access*, vol. 10, no. 8, pp. 83350–83367, 2022.
5. J. C. S. De Morais, R. Gules, J. L. S. De Morais, and L. G. Fernandes, "Transformerless DC-DC converter with high voltage gain based on a switched-inductor structure applied to photovoltaic systems," *Brazilian Power Electronics Conference (COBEP)*, Juiz de Fora, Brazil, 2017.
6. S. N. Choudhary and D. Elangovan, "High gain, naturally clamped DC–DC converter for X-ray application," in *Proc. Int. Conf. on Computation of Power, Energy, Information and Communication (ICCPEIC)*, Melmaruvathur, Tamil Nadu, India, 2016.
7. M. Khan and R. Thakre, "Employing a DC-DC converter with two input boost stages to achieve high voltage gain," *IEEE International Conference on Electrical, Instrumentation and Communication Engineering (ICEICE)*, Karur, Tamil Nadu, India, 2017.
8. A. Anto and A. Sunny, "High voltage gain DC-DC converter for DC microgrid," *International Conference on Intelligent Computing, Instrumentation and Control Technologies (ICICICT)*, Kerala, India, 2017.
9. P. Mohammadi and J. S. Moghani, "Double-input high-gain bidirectional DC-DC converter for hybrid energy storage systems in DC-micro grid," *9th Annual Power Electronics, Drives Systems and Technologies Conference (PEDSTC)*, Tehran, Iran, 2018.
10. S. B. Kjaer, J. K. Pedersen, and F. Blaabjerg, "A review of single-phase grid-connected inverters for photovoltaic modules," *IEEE Transactions on Industry Applications*, vol. 41, no. 5, pp. 1292–1306, 2005.
11. M. Ahmadi, E. Galvan, E. Adib, and H. Farzanehfard, "New fully soft switched bi-directional converter for Hybrid Electric Vehicles: Analysis and control," *IECON 36th Annual Conference on IEEE Industrial Electronics Society*, Glendale, Arizona, United States of America, 2010.
12. M. Ahmadi, M. R. Mohammadi, E. Adib, and H. Farzanehfard, "Family of non-isolated zero current transition bi-directional converters with one auxiliary switch," *IET Power Electronics*, vol. 5, no. 2, pp. 158–165, 2012.
13. O. Abutbul, A. Gherlitz, Y. Berkovich, and A. Ioinovici, "Step-up switching-mode converter with high voltage gain using a switched capacitor circuit," *IEEE Transactions on Circuits and Systems I*, vol. 50, no. 8, pp. 1098–1102, 2003.
14. H. Chiu and L. Lin, "A bidirectional DC-DC converter for fuel cell electric vehicle driving system," *IEEE Transactions on Power Electronics*, vol. 21, no. 4, pp. 950–958, 2006.